Received: 26 October 2017 | Accepted: 24 March 2018

DOI: 10.1002/hyp.11516

RESEARCH ARTICLE

WILEY

A multiscaling-based intensity–duration–frequency model for extreme precipitation

Hans Van de Vyver

Royal Meteorological Institute of Belgium, Ringlaan 3, Uccle, Brussels B1180, Belgium

Correspondence
Hans Van de Vyver, Royal Meteorological Institute of Belgium, Ringlaan 3, Uccle, Brussels B1180, Belgium.
Email: hvijver@meteo.be

Funding information
EU's H2020 Research and Innovation Program, Grant/Award Number: 690462

Abstract

Rainfall intensity–duration–frequency (IDF) curves are a standard tool in urban water resources engineering and management. They express how return levels of extreme rainfall intensity vary with duration. The simple scaling property of extreme rainfall intensity, with respect to duration, determines the form of IDF relationships. It is supposed that the annual maximum intensity follows the generalized extreme value (GEV) distribution. As well known, for simple scaling processes, the location parameter and scale parameter of the GEV distribution obey a power law with the same exponent. Although, the simple scaling hypothesis is commonly used as a suitable working assumption, the multiscaling approach provides a more general framework. We present a new IDF relationship that has been formulated on the basis of the multiscaling property. It turns out that the GEV parameters (location and scale) have a different scaling exponent. Next, we apply a Bayesian framework to estimate the multiscaling GEV model and to choose the most appropriate model. It is shown that the model performance increases when using the multiscaling approach. The new model for IDF curves reproduces the data very well and has a reasonable degree of complexity without overfitting on the data.

KEYWORDS

Bayesian estimation, extreme precipitation, IDF curves, model selection, multiscaling

1 | INTRODUCTION

Rainfall intensity–duration–frequency (IDF) curves are a standard tool in urban water resources engineering and management. They aid engineers in the design of sewer systems and the management of water supply. Denote by $I(d)$ the annual maximum average rainfall intensity of duration d, and let $i_T(d)$ be the value of $I(d)$ with return period T. The IDF curves are plots (usually on a logarithmic scale) of $i_T(d)$ against d, for a wide range of return periods T.

A historical overview of developments in modelling and representations of IDF relationships is provided in Durrans (2010). The general IDF relationship of Koutsoyiannis, Kozonis, and Manetas (1998) is taken to be a separable function of d and T,

$$i_T(d) = \frac{a(T)}{b(d)}, \tag{1}$$

where $a(T)$ is determined by the distribution of the extreme intensities, and

$$b(d) = (d+\theta)^{\eta}, \qquad \text{with } \theta \geq 0, \text{ and } 0 < \eta < 1. \tag{2}$$

Theoretical arguments and empirical evidence support the use of the generalized extreme value (GEV) distribution for quantifying risk associated with hydrological extremes (Coles, 2001; Papalexiou & Koutsoyiannis, 2013; Van de Vyver, 2015b).

More recent extensions of the theory of rainfall extremes are based on stationary multifractal representations of rainfall (Veneziano & Furcolo, 2002; Veneziano, Lepore, Langousis, & Furcolo, 2007; Langousis & Veneziano, 2007; Veneziano & Yoon, 2013). In Veneziano et al. (2007), it was found that the separability condition, as reflected by Equation 1, does not hold.

In the context of spatial variability of hydrological processes, Gupta and Waymire (1990) characterized the probabilistic aspects of the spatial process by introducing the hypothesis of simple scaling and multiscaling. Burlando and Rosso (1996) applied the scaling concepts of Gupta and Waymire (1990) to annual maximum series of rainfall depth against duration. Furthermore, they used the scaling model to derive depth–duration–frequency relationships including the log-normal probability distribution. Next, Menabde, Seed, and Pegram (1999) showed that for location-scale families of cumulative probability distributions for the annual maximum, Equation 1 can be directly derived from the assumption that the annual rainfall maximum is simple scaling. In particular, they constructed IDF curves by considering the Gumbel distribution. Simple scaling GEV models are now widely used for the construction of IDF curves, see Bougadis and Adamowski (2006), Nguyen, Nguyen, and Wang (1998), Van de Vyver (2015a), and Yu, Yang, and Lin (2004) to name a few.

In this paper, we present a multiscaling-based GEV model. It turns out that the corresponding IDF relationship violates the separability condition (Equation 1). We apply the Bayesian framework developed in Van de Vyver (2015a) for appropriate inference. Model selection criteria, to compare the simple scaling and the multiscaling GEV models, are suitably adapted for the present Bayesian approach.

2 | SCALING PROPERTIES OF PRECIPITATION

Let $R_l(d)$ be the total amount of rainfall (mm) for the time interval $[t_l-d,t_l]$ (time expressed in hr) and $I_l(d)=R_l(d)/d$ (mm/hr) the average intensity. We denote by $I_1(d),I_2(d),\ldots$, the series of d-hourly intensity, with time resolution $\Delta=t_l-t_{l-1}$ (e.g., 5 or 10 min), and which contains $N_y=8760/\Delta$ values per year. Then, we consider the series of annual maximum intensity

$$I(d)=\max\{I_1(d),I_2(d),\cdots,I_{N_y}(d)\}. \tag{3}$$

The main assumption in simple scaling models is that the probabilistic properties of the maximum precipitation intensity observed at two different timescales, d and λd, are related with a power law:

$$I(\lambda d)\overset{\text{distr}}{=}\lambda^{-\eta}I(d),\qquad \text{with } 0<\eta<1. \tag{4}$$

This property is called *strict sense simple scaling* by Gupta and Waymire (1990) and Burlando and Rosso (1996). Equation 4 implies that the raw q-order moments obey the power law

$$E[I^q(\lambda d)]=\lambda^{-\alpha_q}E[I^q(d)],\qquad \text{with } \alpha_q=q\eta, \tag{5}$$

which is called *wide-sense simple scaling*. It is often considered as a suitable working assumption in IDF analysis (Bougadis & Adamowski, 2006; Menabde et al. 1999; Nguyen et al. 1998; Yu et al. 2004). However, deviations from simple scaling are to be expected for complex physical processes. Accordingly, Gupta and Waymire (1990) defined multiscaling as

$$E[I^q(\lambda d)]=\lambda^{-\alpha_q}E[I^q(d)],\qquad \text{with } \alpha_q=q\varphi_q\eta, \tag{6}$$

where φ_q is called the dissipation function, and describes the departure from simple scaling.

3 | A GEV SCALING MODEL OF IDF RELATIONSHIPS

We assume that the annual maximum intensity, $I(d)$, follows the GEV distribution. This is related to the statistical behaviour of block maxima,

$$Z=\max\{X_1,\cdots,X_N\}, \tag{7}$$

where $X_1,\ldots,X_N$ is a sequence of independent and identically distributed random variables (Coles, 2001). If there exist sequences of constants $a_N>0$, and b_N, such that the cumulative distribution of the normalized maximum, $\Pr\{(Z-b_N)/a_N\le z\}$, converges to a nondegenerate limit distribution $G(z)$, as $N\to\infty$, then $G(z)$ is a member of the GEV family:

$$G(z;\mu,\sigma,\xi)=\exp\left[-\left(1+\xi\frac{z-\mu}{\sigma}\right)^{-1/\xi}\right]. \tag{8}$$

For sufficiently large N, one can assume that $\Pr\{Z\le z\}\approx G(z;\mu,\sigma,\xi)$, although one cannot exclude that the convergence may be slow. The location parameter (μ) presents the centre of the distribution, the scale parameter ($\sigma>0$) presents the size of deviations in the location parameter, and the shape parameter (ξ) describes the tail of the distribution. We shortly denote $Z\sim\text{GEV}[\mu,\sigma,\xi]$.

Note that the identically distributed assumption is not met in any real-world case. However, a substantial section of the classical textbook (Leadbetter, Lindgren, & Rootzén, 1983) has been directed towards showing that the classical theory of extremes still applies, under specified general assumptions, to a wide variety of dependent sequences.

For 1-year blocks, the return period T (year) of an extremal event $Z>z$ is, as usual, given by

$$T=\frac{1}{1-G(z)}. \tag{9}$$

Conversely, the T-year return level is

$$z_T=\mu-\frac{\sigma}{\xi}\left\{1-\left[-\log\left(1-\frac{1}{T}\right)\right]^{-\xi}\right\}. \tag{10}$$

The mean and variance of the GEV distribution are given by

$$\begin{aligned}
E[Z] &= \begin{cases} \mu+\sigma\dfrac{\Gamma(1-\xi)-1}{\xi}, & \text{if } \xi\neq 0,\ \xi<1,\\ \mu+\sigma\gamma, & \text{if } \xi=0,\\ \infty, & \text{if } \xi\ge 1,\end{cases}\\
\text{Var}[Z] &= \begin{cases} \sigma^2\dfrac{g_2-g_1^2}{\xi^2}, & \text{if } \xi\neq 0,\ \xi<\dfrac{1}{2},\\ \sigma^2\dfrac{\pi^2}{6} & \text{if } \xi=0,\\ \infty, & \text{if } \xi\ge\dfrac{1}{2},\end{cases}
\end{aligned} \tag{11}$$

where $g_k=\Gamma(1-k\xi)$, in which $\Gamma(.)$ is the gamma function, and γ is Euler's constant.

In the above notation, we have

$$I(d)\sim \mathrm{GEV}[\mu(d),\sigma(d),\xi(d)], \tag{12}$$

where $\mu(d)$ and $\sigma(d)$ depend on d and where $\xi(d)=\xi$ is usually kept constant (Koutsoyiannis et al., 1998; Nguyen et al., 1998; Van de Vyver, 2015a). The parameters $\mu(d)$ and $\sigma(d)$ are related to the mean and standard deviation as

$$\mu(d)=E[I(d)]-\frac{g_1-1}{\xi}\sigma(d),\qquad \sigma(d)=\sqrt{\frac{\xi^2}{g_2-g_1^2}\mathrm{Var}[I(d)]}, \tag{13}$$

if $\xi\neq 0$, $\xi<\frac{1}{2}$. Similar expressions hold when $\xi=0$. The case $\xi\geq\frac{1}{2}$ does not need to be considered, because it is expected that ξ lies in a narrow range, approximately from 0 to 0.23 (Papalexiou & Koutsoyiannis, 2013).

3.1 | Simple scaling

Take the scale factor $\lambda=d_0/d$, where d_0 is a reference duration. Following Burlando and Rosso (1996), we get

$$E[I(d)]=d^{-\eta}a_1,\qquad \mathrm{Var}[I(d)]=d^{-2\eta}V^2a_1^2, \tag{14}$$

with $a_1=d_0^{\eta}E[I(d_0)]$, and V the coefficient of variation, which is independent of duration d:

$$V=\sqrt{\mathrm{Var}[I(d)]/E^2[I(d)]}=\sqrt{\mathrm{Var}[I(d_0)]/E^2[I(d_0)]}. \tag{15}$$

By substituting the mean and the variance (Equation 14), in Equation 13, one obtains the four-parameter simple scaling GEV model, $I(d)\sim\mathrm{GEV}[\mu(d),\sigma(d),\xi]$:

$$\mu(d)=d^{-\eta}\mu,\qquad \sigma(d)=d^{-\eta}\sigma,\qquad \text{with}\qquad 0<\eta<1, \tag{16}$$

where $\mu:=d_0^{\eta}\mu(d_0)$ and $\sigma:=d_0^{\eta}\sigma(d_0)$. Denote by $\psi=(\mu,\sigma,\xi,\eta)$ the vector of parameters where (μ,σ,ξ) are the GEV distribution parameters for hourly precipitation (d_0=1 hr), and η parameterizes the simple scaling property. The model was already derived in Nguyen et al. (1998), and for the Gumbel distribution (ξ=0), in Menabde et al. (1999).

The T-year return level of extreme d-hourly intensity can be computed by means of Equation 10. For the GEV model (Equation 16), we get

$$\begin{aligned} i_T(d) &= d^{-\eta}\mu-\frac{d^{-\eta}\sigma}{\xi}\left\{1-\left[-\log\left(1-\frac{1}{T}\right)\right]^{-\xi}\right\} \\ &= \frac{\mu-\frac{\sigma}{\xi}\left\{1-\left[-\log\left(1-\frac{1}{T}\right)\right]^{-\xi}\right\}}{d^{\eta}}, \end{aligned} \tag{17}$$

which has essentially the same form as the general IDF relationship (Equation 1) when θ=0. The θ parameter is only relevant for IDF relationships including a minimum duration smaller than 1 hr. As illustrated in Koutsoyiannis et al. (1998), the IDF curves become approximately straight lines in the logarithmic plot for $d\geq 1$ hr. A similar observation was also made with the Uccle series (Van de Vyver, 2015a). Furthermore, model selection criteria in a Bayesian framework suggested that the simplification θ=0 in Equation 1 should be strongly preferred, if we are concerned with durations $d\geq 1$ hr.

3.2 | Multiscaling

The mean and the variance take the form

$$E[I(d)]=d^{-\eta}a_1,\qquad \mathrm{Var}[I(d)]=d^{-2\varphi_2\eta}a_2-d^{-2\eta}a_1^2, \tag{18}$$

with $a_2=d_0^{2\varphi_2\eta}E[I^2(d_0)]$. As in Burlando and Rosso (1996), the requirement of φ_q to be concave yields a constraint in the model derivation, so we have $\varphi_2\geq 1$.

Similar to the simple scaling model, one can substitute Equation 18 in Equation 13, and the resulting GEV model has five parameters, that is, a_1, a_2, η, φ_2, and ξ. Unfortunately, small perturbations in φ_2 result in relatively large changes in the variance. As a result, the maximum likelihood estimator is highly variable. In general, problems that are highly sensitive to initial conditions, or data, are called ill-posed and should be reformulated for numerical treatment. The key of the solution is to approximate the variance in Equation 18 by only one term. The model reformulation will be approximative, because the difference (or sum) of power functions, appearing in $\mathrm{Var}[I(d)]$, cannot be simplified any further.

For two different powers $s_1\leq s_2$, which are sufficiently close together, we may assume that, to a good approximation,

$$m_1d^{s_1}+m_2d^{s_2}\approx(m_1+m_2)d^{s^*},\quad \text{with}\ s_1\leq s^*\leq s_2,\qquad \text{for}\ m_{1,2}>0. \tag{19}$$

For φ_2 values close to 1, we apply Equation 19 to Equation 18, to get an approximative scaling law for $\mathrm{Var}[I(d)]$:

$$\mathrm{Var}[I(d)]\approx d^{-2\eta_2}c_2,\qquad \text{where}\ c_2=a_2-a_1^2,\qquad \text{and}\ \eta_2\geq\eta, \tag{20}$$

or equivalently, when choosing d_0=1 hr,

$$\mathrm{Var}[I(d)]\approx d^{-2\eta_2}\mathrm{Var}[I(1)],\qquad \text{with}\ \eta_2\geq\eta. \tag{21}$$

We have examined 10-min data sets (see Section 5 for data description) for log–log linearity of the variance versus duration (Figure 1). As expected, deviations from a straight line are generally larger as for the first two raw moments, but the scaling of the variance may nonetheless serve as a reasonable working hypothesis.

Proceeding in an analogous way, it follows from Equations 13 and 21 that $\sigma(d)\approx d^{-\eta_2}\sigma$, where σ is the scale parameter for hourly precipitation. Similarly, considering the first equation in Equation 13, one can argue that $\mu(d)\approx d^{-\eta_1}\mu$, where μ is the location parameter for hourly precipitation. In addition, we have two possibilities: (a) $\eta_1\leq\eta\leq\eta_2$ or (b) $\eta_2\leq\eta\leq\eta_1$. In Equation 20, we obtained $\eta_2\geq\eta$ so that only (a) is possible. In conclusion, we have proved that $\eta_1\leq\eta_2$. Additional constraints can be made from empirical evidence. For example, it is observed worldwide that $\mu(d_1)>\mu(d_2)$ for $d_1<d_2$, yielding the constraint $0<\eta_1$. Unfortunately, we were not able to prove $\eta_2<1$, but because all the powers involved (i.e., $\eta_{1,2}$, η, and $\varphi_2\eta$) are assumed to be close to each other, it is likely that $\eta_2<1$, and if it is not the case, η_2 cannot largely exceed 1.

We illustrate the theory with a preliminary analysis. Figure 2 shows a log–log plot of the GEV parameters ([a] location and [b] scale) against duration. The slope estimator for the scaling exponents gives $\hat{\eta}_1=0.724$ and $\hat{\eta}_2=0.845$. However, such an estimator is not able to decide whether the differences in $\hat{\eta}_1$ and $\hat{\eta}_2$ are significant. A rigorous statistical methodology is proposed in Section 4.

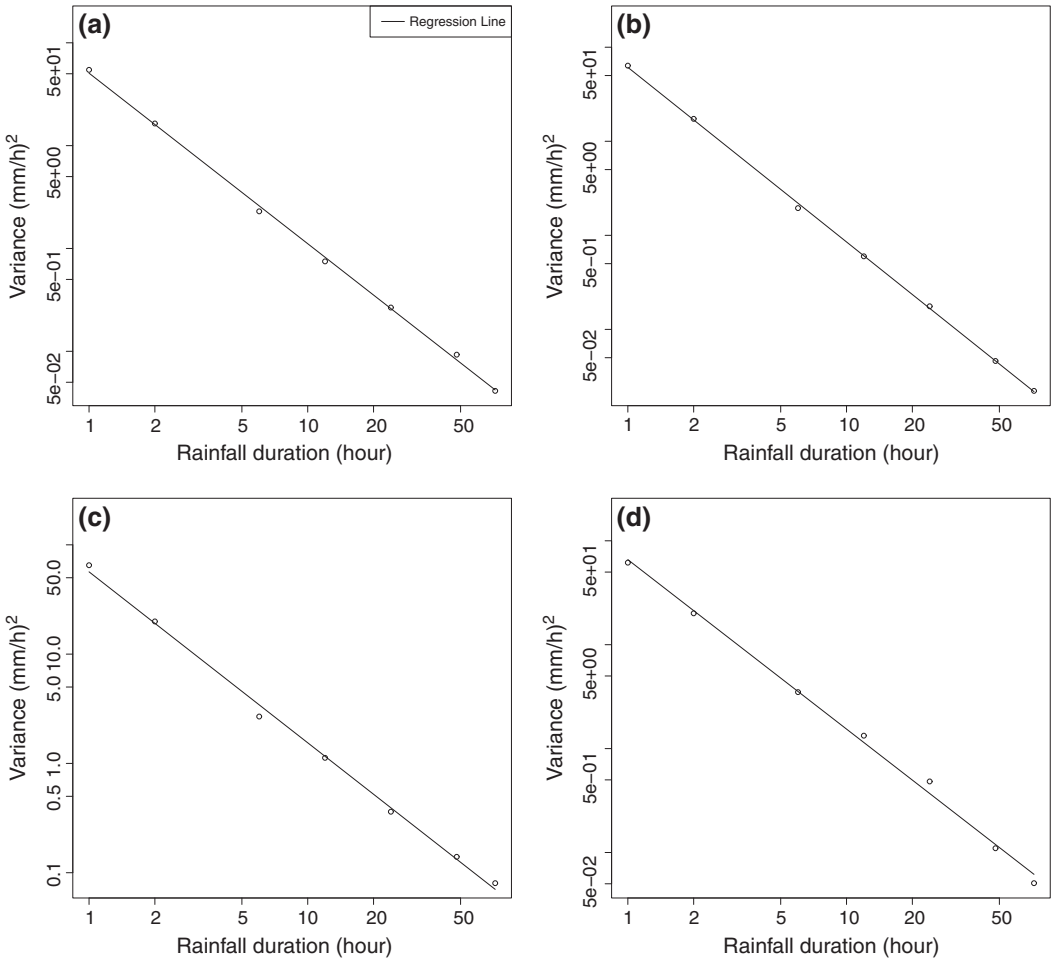

FIGURE 1 The variance, VAR[$I(d)$], as a function of duration d. Stations are (a) Uccle, (b) Wasmuel, (c) Spa, and (d) Raversijde

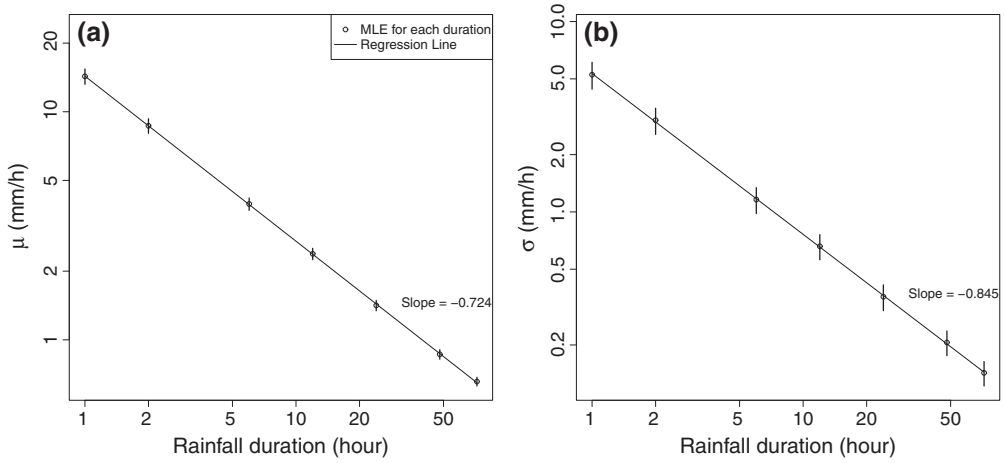

FIGURE 2 GEV parameters plotted against duration d (logarithmic scale). (a) Location parameter μ and (b) scale parameter σ. The vertical lines represent the 95% confidence interval. Station Uccle (Belgium). MLE = maximum likelihood estimator

To summarize, the above may suggest a five-parameter GEV model, $I(d)$~GEV[$\mu(d), \sigma(d), \xi$]:

$$\mu(d) = d^{-\eta_1}\mu, \quad \sigma(d) = d^{-\eta_2}\sigma, \qquad \text{with } 0<\eta_1 \le \eta_2, \qquad \text{and } \eta_1<1. \quad (22)$$

Denote by $\psi=(\mu, \sigma, \xi, \eta_1, \eta_2)$ the vector of parameters where (μ, σ, ξ) are the GEV distribution parameters for hourly precipitation (d_0=1 hr), and (η_1, η_2) characterizes the scaling of $\mu(d)$ and $\sigma(d)$ against d. It extends the simple scaling GEV model (Equation 16). Strictly speaking, the simplified GEV model (Equation 22) is not multiscaling, because the derivation is of an approximative nature, and should destroy the multiscaling property. Later, in Section 6, we demonstrate that the multiscaling property is satisfied to a very good approximation.

Remark that the corresponding T-year return level of extreme d-hourly intensity,

$$i_T(d) = d^{-\eta_1}\mu - \frac{d^{-\eta_2}\sigma}{\xi}\left\{1-\left[-\log\left(1-\frac{1}{T}\right)\right]^{-\xi}\right\}, \tag{23}$$

cannot be written in the form of the general IDF relationship (Equation 1), or in other words, there is no separable functional dependence on T and d.

In Veneziano and Furcolo (2002), Veneziano et al. (2007), Langousis and Veneziano (2007), and Veneziano and Yoon (2013), the scaling of IDF curves was derived under the assumption of multifractality of the rainfall process, rather than multifractality of the annual maxima. It should be noted that both assumptions are different. We will compare the IDF values produced by the new model and an earlier model of Veneziano et al. (2007) in Section 6.

4 | INFERENCE FOR IDF MODELS

4.1 | Independence likelihood

Consider an m-dimensional random vector Y, with probability density $g(y;\psi,\varphi)$, where ψ and φ parameterize the marginal structure and the dependence, respectively. For n independent replicates of Y, denoted by $\mathbf{y} = (y_{jk}) \in \mathbb{R}^{n\times m}$, the *full likelihood* is

$$L(\mathbf{y};\psi,\varphi) = \prod_{j=1}^{n} g(y_{j1},\cdots,y_{jm};\psi,\varphi). \tag{24}$$

In many cases, the joint density function $g(.;\psi,\varphi)$ is analytically unknown, or computationally prohibitive. A commonly used approach to statistical inference for clustered data is to fit models as thought the observations are independent and then to adjust the errors to take account for the dependence (Chandler & Bate, 2007). The resulting *independence likelihood* is

$$L_{\text{ind}}(\mathbf{y};\psi) = \prod_{j=1}^{n}\prod_{k=1}^{m} g(y_{jk};\psi), \tag{25}$$

where $g(.;\psi)$ is the density function of the margins. It belongs to the general class of composite likelihoods (Varin, Reid, & Firth, 2011).

In the present IDF analysis, the matrix of annual maximum intensities is denoted by $\mathbf{i} = (i_j(d_k)) = (i_{jk}) \in \mathbb{R}^{n\times m}$, where j=1,...,n refers to the year and d_k, k=1,...,m to the rainfall duration. In particular, we selected commonly used durations in IDF analysis: 1, 2, 6, 12, 24, 48, and 72 hr. It is assumed that the yearly observation $(i_{j1},\ldots,i_{jm})$ is a realization of the random vector $I=(I(d_1),\ldots,I(d_m))$, where the margins are GEV distributed. Thus, $g(.;\psi)$ in Equation 25 is the density function of GEV$[\mu(d),\sigma(d),\xi]$, and ψ is the vector of marginal parameters. Recall that for simple scaling, $\psi=(\mu,\sigma,\xi,\eta)$, and based on multiscaling, $\psi=(\mu,\sigma,\xi,\eta_1,\eta_2)$.

4.2 | Maximum likelihood estimation

Denote by $\phi=(\psi,\varphi)$ the full set of parameters and $\hat{\phi}$ the maximum likelihood estimator, obtained by maximizing the full log-likelihood $l(\mathbf{y};\phi)=\log L(\mathbf{y};\phi)$. Suppose that the data come from the distribution $g(y;\phi^{(0)})$. The asymptotic properties of the maximum likelihood estimator are well known: as $n\to\infty$ we have, in distribution, $\hat{\phi}\to\mathcal{N}\left(\phi^{(0)}, H(\phi^{(0)})^{-1}\right)$, where H is minus the expected Hessian of l at $\phi^{(0)}$. Similarly, one can define the maximum independence likelihood estimator $\hat{\psi}_{\text{ind}}$, which is also known to be normally distributed (Chandler & Bate, 2007; Davison, 2003; Varin et al. 2011):

$$\hat{\psi}_{\text{ind}} \xrightarrow{\text{distr}} \mathcal{N}\left(\psi^{(0)}, H_{\text{ind}}(\psi^{(0)})^{-1} J_{\text{ind}}(\psi^{(0)}) H_{\text{ind}}(\psi^{(0)})^{-1}\right), \text{ as } n\to\infty, \tag{26}$$

with $H_{\text{ind}}(\psi^{(0)})=-E[\nabla^2 l_{\text{ind}}(\mathbf{y};\psi^{(0)})]$ and $J_{\text{ind}}(\psi^{(0)})=\text{Var}[\nabla l_{\text{ind}}(\mathbf{y};\psi^{(0)})]$. If there is no dependence, we have $H_{\text{ind}}(\psi^{(0)})=J_{\text{ind}}(\psi^{(0)})$.

4.3 | Bayesian inference

In the Bayesian setting, the parameters ϕ are modelled as a random variable. In contrast with the frequentist approach, there is no "true" parameter $\phi^{(0)}$. Suppose that the probability density function $\pi(\phi)$ expresses prior beliefs about ϕ, before some evidence is considered. Given the full likelihood $L(\mathbf{y};\phi)$, Bayes' theorem gives the full posterior density as

$$\pi(\phi|\mathbf{y}) \propto L(\mathbf{y};\phi)\pi(\phi). \tag{27}$$

If a single estimate is required, the mean or the median of the posterior distribution can be used.

Similarly, we use the independence likelihood $L_{\text{ind}}(\mathbf{y};\psi)$ to define the independence posterior density as

$$\pi_{\text{ind}}(\psi|\mathbf{y}) \propto L_{\text{ind}}(\mathbf{y};\psi)\pi_{\text{ind}}(\psi). \tag{28}$$

It can be shown that, under usual regularity conditions, the asymptotic (independence) posterior distribution takes the form (Pauli, Racugno, & Ventura, 2011; Ribatet, Cooley, & Davison, 2012):

$$\begin{aligned}&\pi(\phi|\mathbf{y}) \to \mathcal{N}\left(\phi^{(0)}, H(\phi^{(0)})^{-1}\right),\\ &\pi_{\text{ind}}(\psi|\mathbf{y}) \to \mathcal{N}\left(\psi^{(0)}, H_{\text{ind}}(\psi^{(0)})^{-1}\right), \text{as } n\to\infty.\end{aligned} \tag{29}$$

It can be seen that the asymptotic variance of the full posterior distribution is equal to these of the maximum likelihood estimator. In contrast, the asymptotic variance of the independence posterior is incorrect, because it must be equal to $H_{\text{ind}}(\psi^{(0)})^{-1}J_{\text{ind}}(\psi^{(0)})H_{\text{ind}}(\psi^{(0)})^{-1}$. Pauli et al. (2011) and Ribatet et al. (2012) proposed an adjusted composite likelihood, $L_{\text{adj}}(\mathbf{y};\psi)$, so that the posterior distribution,

$$\pi_{\text{adj}}(\psi|\mathbf{y}) \propto L_{\text{adj}}(\mathbf{y};\psi)\pi(\psi), \tag{30}$$

has the correct variance.

We briefly summarize the main idea. Suppose that ψ contains p elements. Also, assume that the full set of parameters $\phi=(\psi,\varphi)$ contains p^* elements. As well known, we have for the full log-likelihood ratio statistic (Coles, 2001; Davison, 2003):

$$D(\phi^{(0)}) = 2\left[l(\mathbf{y};\hat{\phi}) - l(\mathbf{y};\phi^{(0)})\right] \xrightarrow{\text{distr}} \chi^2_{p^*}, \qquad \text{as } n\to\infty. \tag{31}$$

By comparison with Equation 31, we have for the independence log-likelihood ratio statistic:

$$D_{\text{ind}}(\psi^{(0)}) = 2\left[l_{\text{ind}}(\mathbf{y};\hat{\psi}_{\text{ind}}) - l_{\text{ind}}(\mathbf{y};\psi^{(0)})\right] \xrightarrow{\text{distr}} \sum_{i=1}^{p}\lambda_i X_i, \text{ as } n\to\infty, \tag{32}$$

where $X_1,\ldots,X_p$ are independent χ^2_1 random variables and $\lambda_1,\ldots,\lambda_p$ are the eigenvalues of $H_{\text{ind}}(\psi^{(0)})^{-1}J_{\text{ind}}(\psi^{(0)})$, see Kent (1982). The idea of

Pauli et al. (2011) consists of adjusting the composite likelihood to such a degree that the asymptotic χ^2-distribution for the log-likelihood ratio statistic is preserved, that is,

$$D_{\text{adj}}(\psi^{(0)}) = 2\left[l_{\text{adj}}(\mathbf{y};\hat{\psi}_{\text{ind}}) - l_{\text{adj}}(\mathbf{y};\psi^{(0)})\right] \xrightarrow{\text{distr}} \chi^2_p, \qquad \text{as } n\to\infty, \quad (33)$$

where $l_{\text{adj}} = \log L_{\text{adj}}$. Two adjustments are currently known:

- *Magnitude adjustment* (Pauli et al. 2011). Determine k,
$$l_{\text{magn}}(\mathbf{y};\psi) = k\, l_{\text{ind}}(\mathbf{y};\psi), \quad (34)$$
in such a way that the first-order moment of $D_{\text{magn}}(\psi^{(0)})$ converges to that of the χ^2_p-distribution, compare Equation 33. We get $k = p/\text{tr}[H^{-1}_{\text{ind}}(\psi^{(0)})J_{\text{ind}}(\psi^{(0)})]$. However, the correct variance of the asymptotic independence posterior is only found when p=1: $[kH_{\text{ind}}(\psi^{(0)})]^{-1} = H_{\text{ind}}(\psi^{(0)})^{-1}J_{\text{ind}}(\psi^{(0)})H_{\text{ind}}(\psi^{(0)})^{-1}$. Anyway, Pauli et al. (2011) argued that for p>1, the adjusted variance is much more suited than the unadjusted one.
- *Curvature adjustment* (Ribatet et al. 2012). Determine $C \in \mathbb{R}^{p\times p}$ in
$$l_{\text{curv}}(\mathbf{y};\psi) = l_{\text{ind}}(\mathbf{y};\psi^*), \qquad \psi^* = \hat{\psi}_{\text{ind}} + C(\psi - \hat{\psi}_{\text{ind}}), \quad (35)$$
such that Equation 33 holds.

4.4 | Model comparison

We consider two popular model selection criteria: the Akaike information criterion (AIC) and the Bayesian information criterion (BIC). Modifications of AIC and BIC are easily derived in the general framework of composite likelihoods (Gao & Song, 2010; Varin & Vidoni, 2005; Varin et al., 2011). For maximum independence likelihood estimation, they have the usual forms $\text{AIC} = -2l_{\text{ind}}(\mathbf{y};\hat{\psi}_{\text{ind}}) + 2p_D$ and $\text{BIC} = -2l_{\text{ind}}(\mathbf{y};\hat{\psi}_{\text{ind}}) + p_D \log n$, where p_D is the effective number of parameters, evaluated as $p_D = \text{tr}[J_{\text{ind}}(\hat{\psi})H_{\text{ind}}(\hat{\psi})^{-1}]$. It can be seen that AIC and BIC reward goodness-of-fit (as assessed by the likelihood function), but they penalize the complexity of the model. We choose the model with the lowest AIC or BIC value.

In the context of Bayesian inference from composite likelihoods, analogues of AIC and BIC are not derived yet. Concerning the likelihood contribution in AIC and BIC, $\hat{\psi}_{\text{ind}}$ may be replaced by the posterior mean, $\bar{\psi}_{\text{ind}}$. For the computation of p_D, we follow Spiegelhalter, Best, Carlin, and van der Linde (2002) who formed a basis for classical and Bayesian measures of model dimensionality. From a Bayesian perspective, they defined the excess of the true over the estimated residual information as

$$D = -2l(\mathbf{y};\phi) + 2l(\mathbf{y};\bar{\phi}), \quad (36)$$

where ϕ is a random vector of parameters and $\bar{\phi}$ a point estimate for ϕ. The effective number of parameters, p_D, can be estimated by the posterior expectation of D, with respect to $\pi(\phi|\mathbf{y})$:

$$p_D = E_{\phi|\mathbf{y}}[-2l(\mathbf{y};\phi) + 2l(\mathbf{y};\bar{\phi})]. \quad (37)$$

For a model with large sample size, p_D is equal to the number of parameters. This can be seen as follows: For sufficiently large sample size, one can assume that

$$\pi(\phi|\mathbf{y}) \approx \mathcal{N}(\hat{\phi}, H(\hat{\phi})^{-1}) \quad (38)$$

holds, where $\bar{\phi} = \hat{\phi}$, such that the posterior covariance $J(\hat{\phi}) = 0$ (Bernardo & Smith, 1994; Spiegelhalter et al., 2002). Taylor expansion of D around $\hat{\phi}$ results in

$$D \approx (\phi - \hat{\phi})^T H(\hat{\phi})^{-1}(\phi - \hat{\phi}) \overset{\text{distr}}{=} \chi^2_p, \quad (39)$$

and by taking the expectation with respect to $\pi(\phi|\mathbf{y})$, we get $p_D = p^*$, as $n\to\infty$. For composite likelihoods, Equation 37 is not valid, and we have to replace the likelihood by the adjusted likelihood in Equation 36. We get

$$D_{\text{adj}} = -2l_{\text{adj}}(\mathbf{y};\psi) + 2l_{\text{adj}}(\mathbf{y};\bar{\psi}_{\text{ind}}), \quad (40)$$

which is, by construction, (approximately) χ^2_p-distributed, as $n\to\infty$. Thus, a measure for the number of effective parameters is the expectation of D_{adj} with respect to the adjusted posterior:

$$p_D = E_{\psi_{\text{adj}}|\mathbf{y}}[-2l_{\text{adj}}(\mathbf{y};\psi_{\text{adj}}) + 2l_{\text{adj}}(\mathbf{y};\bar{\psi}_{\text{ind}})]. \quad (41)$$

To summarize, analogues of AIC and BIC for Bayesian independence likelihoods are

$$\text{AIC} = -2l_{\text{ind}}(\mathbf{y};\bar{\psi}_{\text{ind}}) + 2p_D, \text{ and } \text{BIC} = -2l_{\text{ind}}(\mathbf{y};\bar{\psi}_{\text{ind}}) + p_D \log n, \quad (42)$$

where p_D is given by Equation 41.

4.5 | Implementation

Prior distributions of the GEV parameters are similar to those of Van de Vyver (2015a; table 3):

$$\mu \sim \mathcal{N}(0, 10^4), \quad \sigma \sim \ln\mathcal{N}(0, 10^4), \quad \xi \sim \text{Beta}(\alpha = 6, \beta = 9, -0.5, 0.5). \quad (43)$$

The prior distributions of the scaling parameters are subject to conditions, $0<\eta<1$, $0<\eta_1\le\eta_2$, and $\eta_1<1$:

- *Simple scaling:* $\eta \sim$ unif. on (0,1),
- *Multiscaling-based:* $(\eta_1,\eta_2) \sim$ bivar. indep. unif. on $\{(\eta_1,\eta_2) \in (0,1)\times(0,2) | \eta_1 \le \eta_2\}$.

The constraint $\eta_2 < l_2$, with l_2=2, is rather arbitrary. The choice of different l_2 values ($l_2 \ge 1$) results, however, to very similar posterior distributions (not shown).

Approximate draws $\psi^{(1)}, \psi^{(2)}, \ldots$ from the posterior distribution are obtained with a Gibbs sampler (Gelman et al. 2013). This in turn consists of Metropolis–Hastings steps to update each parameter of the model. We partition the sampling of the parameters ψ into two blocks ψ_1 and ψ_2:

$$\psi_1 = (\mu,\sigma,\xi), \qquad \text{and } \psi_2 = \begin{cases} \eta, & \text{(simple scaling)}, \\ (\eta_1,\eta_2), & \text{(multiscaling-based)}. \end{cases} \quad (44)$$

Each Monte Carlo Markov chain (MCMC) step begins with an initial value for each model parameter $\psi^{(t)} = (\psi_1^{(t)}, \psi_2^{(t)})$, and then the blocks are successively updated, conditionally on the other block. We use a Metropolis–Hastings step to update a block $\psi_1^{(t)}$ by drawing a value ψ_1^* from a candidate density. The acceptance rate of the proposed value is given by

$$\alpha^{(t)} = \min\left\{1, \frac{L_{\text{adj}}(\mathbf{i};\psi_1^*,\psi_2^{(t)})\pi(\psi_1^*)}{L_{\text{adj}}(\mathbf{i};\psi_1^{(t)},\psi_2^{(t)})\pi(\psi_1^{(t)})}\right\}, \quad (45)$$

and similar for the update of $\psi_2^{(t)}$. Evaluation of one of the adjusted likelihoods (L_{magn} or L_{curv}) requires a preliminary maximization of the independence likelihood to estimate the matrices $H_{ind}(\psi^{(0)})$ and $J_{ind}(\psi^{(0)})$. Technical details are fully described in Ribatet et al. (2012), and more specifically for IDF analysis, in appendix B of Van de Vyver (2015a).

5 | DATA

We considered the 110-year time series (1898–2007) of 10-min precipitation of the Royal Meteorological Institute of Belgium (Uccle, Brussels). Since 1898, the series was recorded by the same instrument (a Hellmann–Fuess pluviograph) and at the same location (Demarée, 2003). In addition, we considered 15 other Belgian pluviograph stations, which also provided 10-min measurements, but for a much shorter period (1967–2004). Some of these series display long periods with missing data, whereas the Uccle series is complete. See Figure 3 for the station locations. For the purpose of this study, we extracted the annual maxima of sliding 10-min aggregated precipitation depths over seven durations: 1, 2, 6, 12, 24, 48, and 72 hr. Next, maximum precipitation depths are easily converted to maximum intensities.

However, if the amount of missing values is high, it will result in underestimated maxima. We used the selection criteria of Papalexiou and Koutsoyiannis (2013) to decide whether or not an annual maximum of an incomplete year should be excluded from the study. For a particular rainfall duration, an annual maximum value is considered as missing if (a) it belongs to the 40% of the lowest values and (b) the amount of missing values is larger than or equal to one third. Next, a given year is considered as missing if at least three of the seven durations are missing. Finally, the data availability of each station is summarized in Table 1.

TABLE 1 Number of withheld annual maxima, for each rainfall duration and pluviograph station

Station	1 hr	2 hr	6 hr	12 hr	24 hr	48 hr	72 hr
Rochefort	37	37	37	37	37	37	37
Forges	36	36	36	36	36	35	34
Dourbes	35	35	35	35	34	34	34
Nadrin	37	37	37	37	37	37	36
Uccle	110	110	110	110	110	110	110
Melle	37	37	37	37	37	37	37
Lacuisine	37	37	37	37	37	37	36
Wasmuel	36	36	36	36	36	36	35
Ernage	31	31	31	31	31	31	31
St Hubert	38	38	38	38	38	38	38
Bierset	38	38	38	38	38	38	38
Spa	37	37	37	37	37	37	37
Deurne	38	38	38	38	38	38	38
Gosselies	34	34	34	33	33	33	33
Florennes	38	38	38	38	38	38	38
Raversijde	38	38	38	38	38	38	38

We examined whether the spatial dependence of the annual maxima is significant. Ideally, cross-correlations are small or negligible, otherwise the extra pluviograph stations (in addition to the Uccle series) may not provide support for identifying the new model. For rainfall durations smaller than 12 hr, the number of pairs that accepted the hypothesis that the correlation is 0 is higher than 90%. Of course, for larger durations, the spatial dependence will be higher; the acceptance rate is ranging between 40% (d=24 hr) and 80% (d=72 hr), but it is only of importance for distances smaller than 100–150 km. Anyway, because the spatial correlation between the stations is negligible for a wide range of durations (up to 12 hr), we can use the extra pluviograph stations to validate the multiscaling-based model.

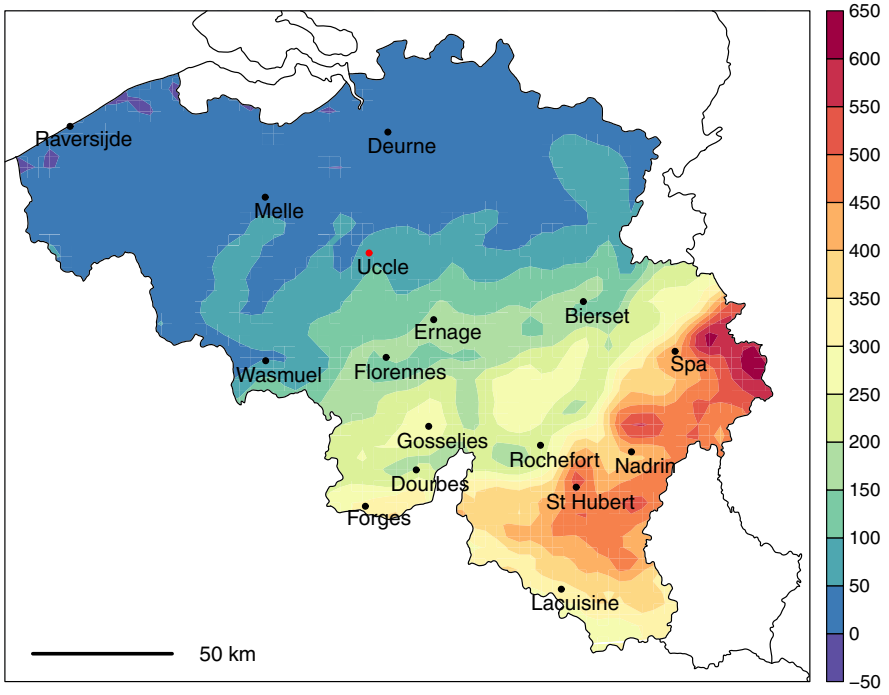

FIGURE 3 Elevation map (m) of Belgium, together with the location of the 10-min pluviograph stations

A necessary condition is that the annual maximum values fit the GEV distribution for any given duration d. A goodness-of-fit assessment was made with reference to the observed rainfall intensity data (d=1,...,72 hr) by means of probability plots and quantile plots. The results (not shown) lend support to the GEV model.

6 | RESULTS

First, we examined the possible loss in accuracy caused by the simplification of the final GEV model (Equation 22). Recall that there are, in fact, two versions of the GEV model: (a) the first version includes the expressions of the mean and the variance under the multiscaling hypothesis, see Equation 18, and (b) a simplified and more practical version, Equation 22. Both versions have five parameters, so we can use the minimized negative log-likelihood values to compare the accuracy (Table 2). Because the likelihood estimator for the original model is unstable, we generated 10^5 random initial values of $(a_1, a_2, \eta, \varphi_2, \xi)$ for the input of the optimization routine, and we kept the smallest minimized negative log-likelihood. We observe that, remarkably enough, the simplified model is more accurate. In conclusion, there are no benefits attached to the original formulation.

We investigated to what extend the simplified GEV model meets the multiscaling property. Figure 4 shows a log–log plot of the first four raw moments against the duration, for the Uccle station. The moments of the GEV models can be easily computed analytically. In addition, we plotted the best fitting regression line through the qth-order moments (q=1,...,4). By construction, the regression lines for the simple scaling model fit perfectly. One can see that the moments of the simplified multiscaling method lie close to a straight line. Proceeding in the same way with the other stations, we observed that the bias and the mean absolute error of the linear regression lie within the range (e-20 and e-18) and (e-4 and e-2), respectively. For comparison, the observed moments produced errors that are, on average, 10 times larger.

TABLE 2 Negative log-likelihood values for two versions of the multiscaling GEV model

Station	Version 1	Version 2
Rochefort	332.78	331.07
Forges	395.45	391.32
Dourbes	320.66	319.38
Nadrin	364.91	361.99
Uccle	1,068.61	1,064.09
Melle	341.77	340.12
Lacuisine	410.20	407.96
Wasmuel	293.11	292.50
Ernage	293.17	270.81
St Hubert	366.08	332.51
Bierset	464.82	428.85
Spa	389.99	389.83
Deurne	360.93	357.32
Gosselies	307.07	305.99
Florennes	369.70	368.47
Raversijde	378.85	377.40

Note. Version 1: including the mean and the variance under the multiscaling hypothesis, see Equation 18. Version 2: simplification of Version 1, see Equation 22.

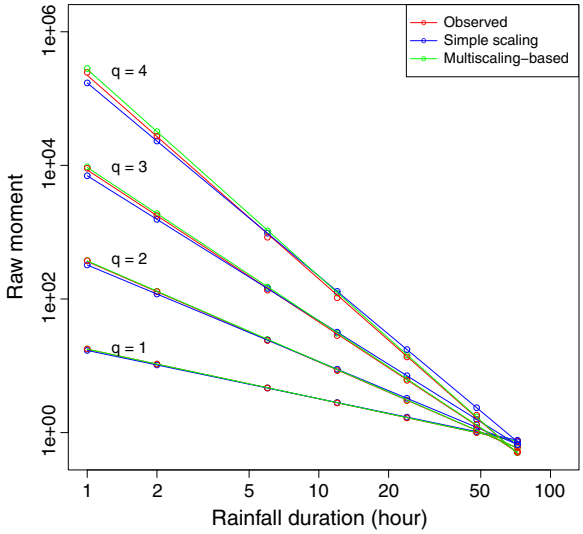

FIGURE 4 Scaling of raw moments, $E[I^q(d)]$, with duration d. Simple scaling GEV model: Equation 16. Multiscaling-based GEV model: Equation 22. Station Uccle (Belgium)

In what follows, we only consider GEV models (Equations 16 and 22). The statistical models were run for 10^5 MCMC iterations, after discarding the first 1,000 iterations to allow for burn-in. The posterior densities from the multiscaling-based model (Figure 5, Uccle) show that there is almost no difference in the magnitude- and curvature-adjusted posteriors. From Figure 5d, it can be seen that the posterior density of η_2 is much wider than that of η_1, and that they overlap by only a small fraction.

Inference results for all the stations and models are listed in Table 3 (magnitude adjusted) and Table 4 (curvature adjusted). There is hardly any difference between the means of the magnitude- and curvature-adjusted posterior. On the other hand, p_D depends on the choice of the adjustment. The posterior means $\bar{\eta}$ and $\bar{\eta}_1$ differ little, and they vary in the narrow range of 0.64–0.75. The posterior mean $\bar{\eta}_2$ lies approximately within the range 0.75–0.87. For Uccle precipitation, the p_D values are closest to the number of parameters. The other series contain less data so that the parameter constraints, in the form of prior information, become more dominant. As a result, the p_D values are generally smaller. In any case, the AIC and BIC scores are lower for the multiscaling-based model. The biggest difference between the models (in terms of AIC and BIC) is seen for Uccle precipitation, as expected, because the series contains three times more years than the other series. In addition, the biggest differences are mainly present in the southern part of Belgium. Smaller differences in the AIC values, say less than 5, are seen in stations Melle, Gosselies, Spa, Raversijde, and Deurne. Overall, the scores lend to support the multiscaling-based model instead of the simple scaling model.

As we have draws $\psi^{(t)}=(\mu^{(t)}, \sigma^{(t)}, \xi^{(t)}, \eta^{(t)})$ of the simple scaling model, with t=1,...,n_s MCMC iterations, we can obtain draws

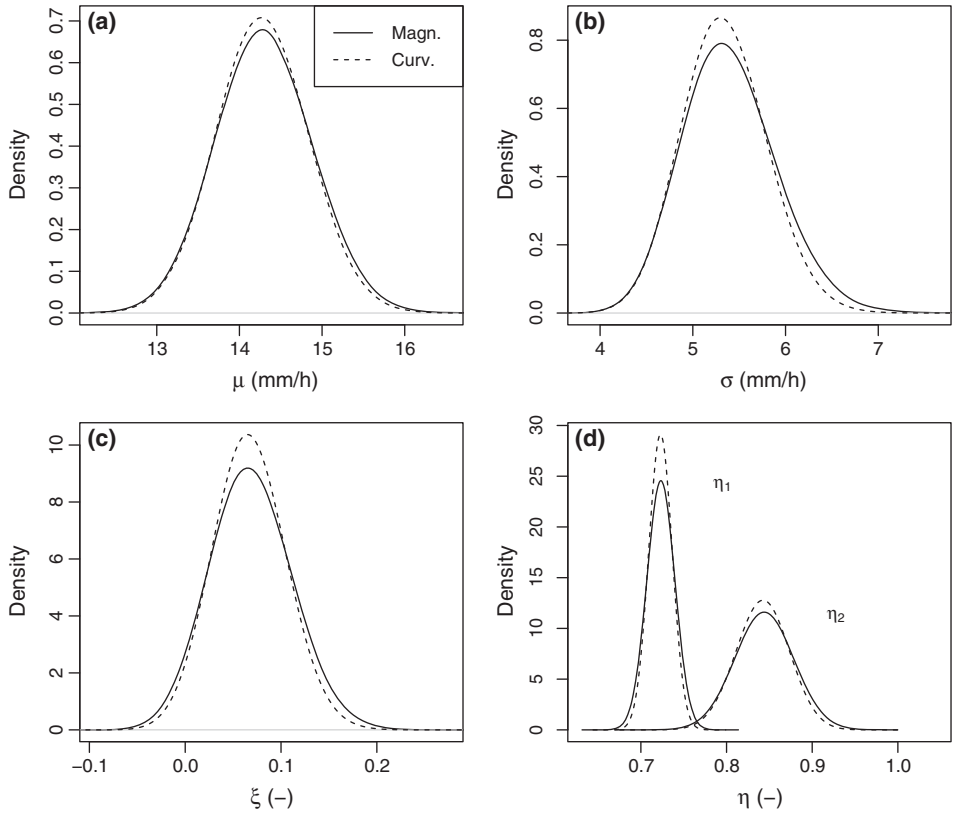

FIGURE 5 Posterior densities of μ, σ, ξ, η_1, and η_2 of the multiscaling-based GEV model. Station Uccle (Belgium)

TABLE 3 Inference results for the scaling GEV models

	Simple scaling				Multiscaling-based				
Station	$\bar{\eta}$	p_D	AIC	BIC	$\bar{\eta_1}$	$\bar{\eta_2}$	p_D	AIC	BIC
Rochefort	0.712	3.49	681.1	686.8	0.718	0.831	4.43	671.6	678.9
Forges	0.702	3.40	812.8	818.4	0.720	0.878	4.45	792.3	799.6
Dourbes	0.691	3.55	656.2	662.0	0.702	0.810	4.27	648.9	655.9
Nadrin	0.691	3.60	753.0	758.9	0.695	0.832	4.44	734.6	741.9
Uccle	0.723	3.85	2,182.5	2,193.0	0.723	0.844	4.79	2,138.2	2,151.3
Melle	0.717	3.65	691.9	697.9	0.715	0.795	4.20	689.6	696.4
Lacuisine	0.637	3.57	844.6	850.5	0.643	0.791	4.51	825.8	833.2
Wasmuel	0.726	3.51	608.9	614.7	0.737	0.876	4.43	594.5	601.8
Ernage	0.730	3.56	559.9	565.4	0.729	0.852	4.36	551.1	557.9
St Hubert	0.653	3.51	693.9	699.7	0.656	0.792	4.54	675.0	682.4
Bierset	0.747	3.57	873.8	879.7	0.750	0.846	4.31	867.1	874.2
Spa	0.666	3.57	793.2	799.0	0.669	0.757	4.28	788.8	795.8
Deurne	0.713	3.62	729.6	735.5	0.711	0.799	4.24	724.5	731.4
Gosselies	0.708	3.50	624.7	630.0	0.715	0.799	4.24	621.4	627.8
Florennes	0.727	3.47	751.8	757.5	0.724	0.824	4.30	746.2	753.2
Raversijde	0.707	3.61	768.8	774.7	0.711	0.794	4.32	764.3	771.4

Note. The magnitude-adjusted independence likelihood was used in the MCMC algorithm.

of the GEV distribution parameters for any duration d_k, that is, $(\mu^{(t)}(d_k), \sigma^{(t)}(d_k), \xi^{(t)}) =: (\mu_k^{(t)}, \sigma_k^{(t)}, \xi^{(t)})$, by means of Equation 16:

$$\mu_k^{(t)} = d_k^{-\eta^{(t)}} \mu^{(t)}, \qquad \sigma_k^{(t)} = d_k^{-\eta^{(t)}} \sigma^{(t)}. \tag{46}$$

Next, for any duration d_k, we obtain corresponding draws from the posterior distribution of the T-year extreme intensity return level, $i_T^{(t)}(d_k) =: i_{T,k}^{(t)}$,

$$i_{T,k}^{(t)} = \mu_k^{(t)} - \frac{\sigma_k^{(t)}}{\xi^{(t)}} \left\{ 1 - \left[-\log\left(1 - \frac{1}{T}\right) \right]^{-\xi^{(t)}} \right\}, \tag{47}$$

TABLE 4 Inference results for the scaling GEV models

	Simple scaling				Multiscaling-based				
Station	$\bar{\eta}$	p_D	**AIC**	**BIC**	$\bar{\eta}_1$	$\bar{\eta}_2$	p_D	**AIC**	**BIC**
Rochefort	0.710	3.58	681.0	686.8	0.717	0.825	4.66	671.8	679.4
Forges	0.706	3.41	813.5	819.1	0.721	0.873	4.64	792.3	799.9
Dourbes	0.687	3.67	655.7	661.8	0.700	0.803	4.49	648.2	655.5
Nadrin	0.689	3.81	752.7	759.0	0.693	0.822	4.77	734.2	742.0
Uccle	0.722	3.91	2,182.4	2,193.2	0.723	0.842	4.89	2,138.1	2,151.6
Melle	0.715	3.79	691.9	698.1	0.714	0.783	4.44	689.4	696.7
Lacuisine	0.635	3.66	844.2	850.2	0.641	0.785	4.67	825.4	833.1
Wasmuel	0.725	3.60	608.8	614.7	0.737	0.871	4.60	594.6	602.1
Ernage	0.727	3.75	559.9	565.7	0.727	0.845	4.67	551.5	558.8
St Hubert	0.649	3.64	693.9	699.9	0.655	0.787	4.67	675.0	682.7
Bierset	0.746	3.69	873.8	879.9	0.750	0.843	4.48	867.0	874.4
Spa	0.665	3.75	793.4	799.5	0.669	0.751	4.52	788.9	796.3
Deurne	0.711	3.76	729.0	735.2	0.711	0.782	4.64	724.5	732.1
Gosselies	0.707	3.60	624.5	630.0	0.716	0.797	4.44	621.3	628.1
Florennes	0.725	3.59	751.7	757.5	0.725	0.817	4.57	746.3	753.8
Raversijde	0.705	3.71	768.6	774.7	0.710	0.784	4.55	764.2	771.6

Note. The curvature-adjusted independence likelihood was used in the MCMC algorithm.

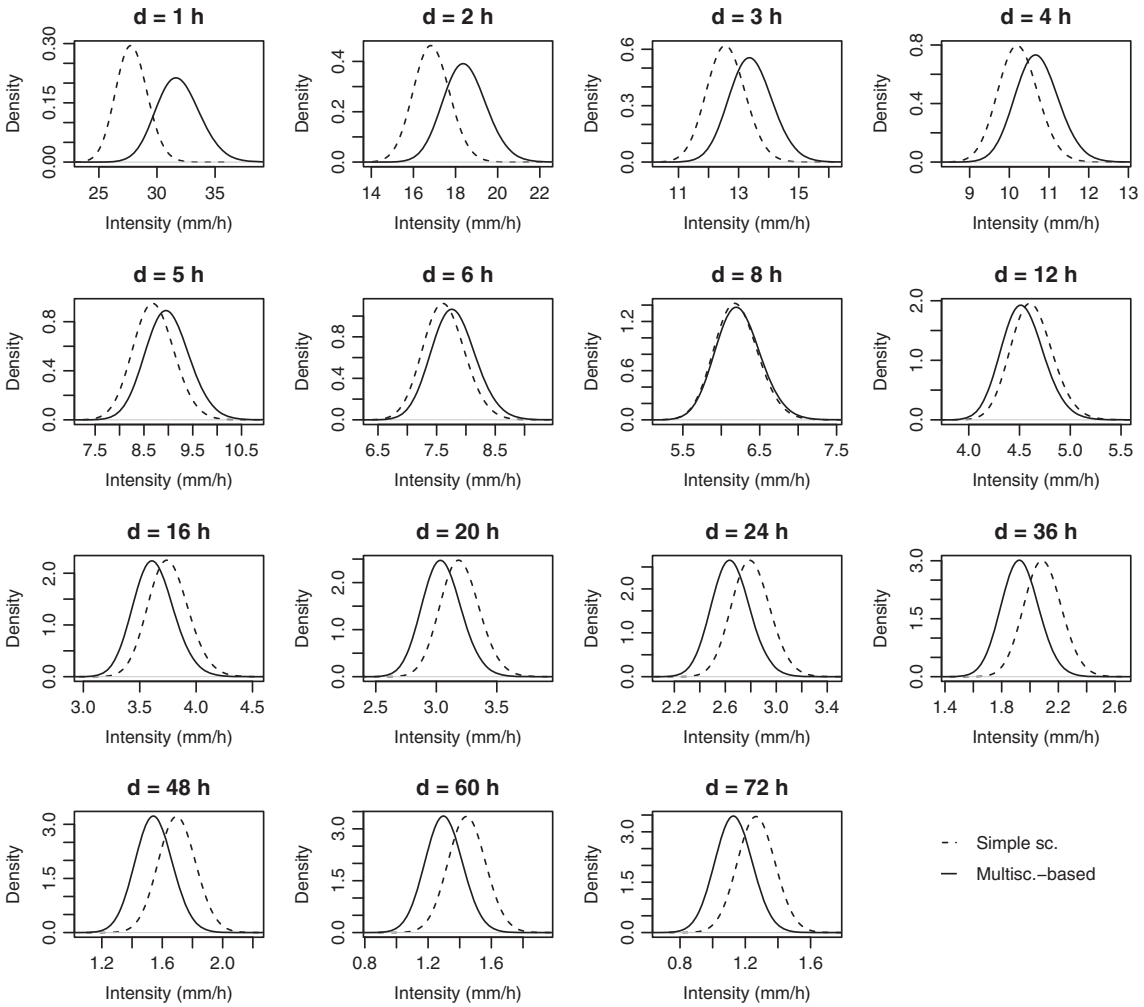

FIGURE 6 Posterior density of 20-year return levels of the maximum intensity. The curvature-adjusted independence likelihood was used in the MCMC. Station Uccle (Belgium)

and similarly for the multiscaling-based model. The posterior mean is estimated directly as

$$\bar{i}_{T,k} = \frac{1}{n_s} \sum_{t=1}^{n_s} i_{T,k}^{(t)}. \quad (48)$$

Figure 6 shows the posterior densities of the 20-year extreme intensity return levels of the simple scaling and multiscaling-based model. Substantial differences between both models are seen for short rainfall durations (say 1–3 hr). For example, the posterior means of the hourly intensity are 27.9 and 31.9 mm for the simple scaling and multiscaling-based model, respectively. The posterior distributions are similar for durations 6–12 hr, and for durations larger than 12 hr, the distributions are, again, starting to differ.

Figure 7 shows a logarithmic plot of the IDF curves in the form of the posterior mean $\bar{i}_{T,k}$ versus d_k, for a range of return periods, T=2, 5, 10, 20, 50, and 100 years. Apart from the curves resulting from the

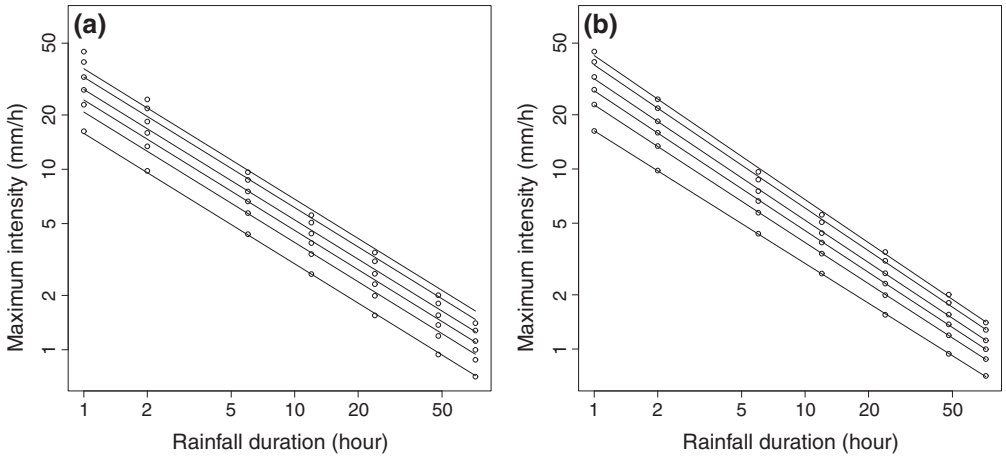

FIGURE 7 Intensity–duration–frequency curves at Uccle (Belgium) for return periods T=2, 5, 10, 20, 50, and 100 years, as obtained by Bayesian inference from the curvature-adjusted independence likelihood. (a) Simple scaling. (b) Multiscaling-based. The dots correspond to the intensities obtained directly from the individually fitted GEV distribution for each duration

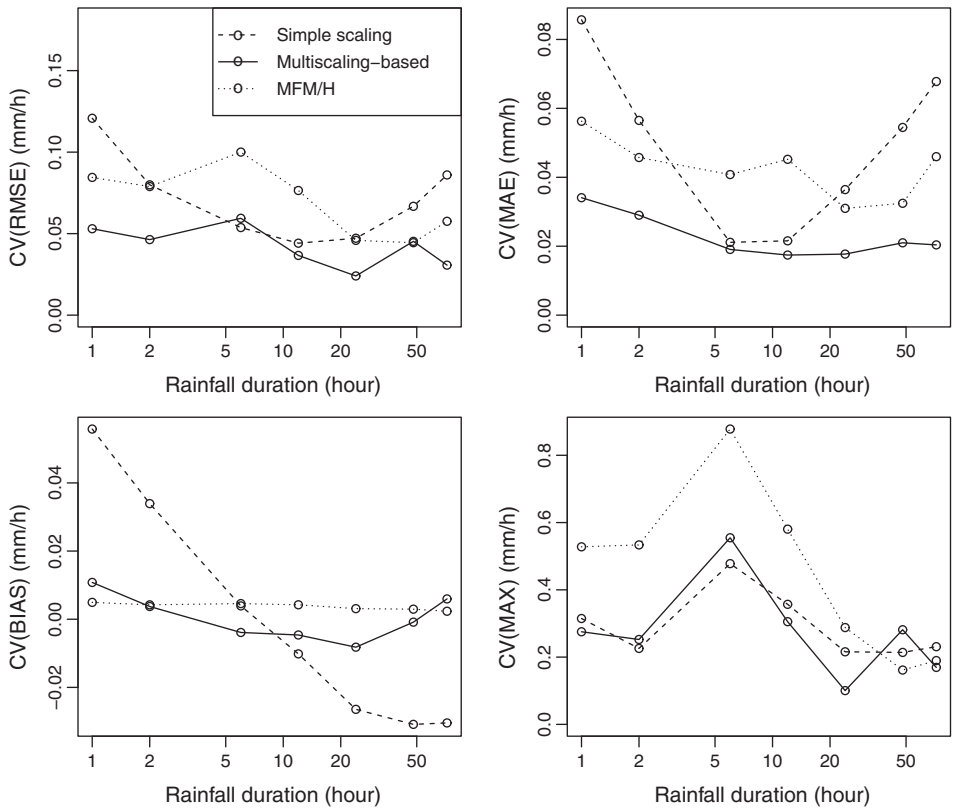

FIGURE 8 Coefficient of variation (CV) of the scores (Equation 49), as a function of the rainfall duration. The curvature-adjusted independence likelihood was used in the Monte Carlo Markov chain algorithm. MFM/H = multifractal marginal and hybrid method (Veneziano et al. 2007). Station Uccle (Belgium)

IDF models (continuous lines), we have also plotted (dots) the intensities obtained directly from the individually fitted GEV distribution for each duration. It can be seen by eye that the IDF curves based on the multiscaling-based model (Figure 7b) are much closer to the dots than for the simple scaling model (Figure 7a).

For assessing the quantitative goodness-of-fit, we used four scores: the root mean square error (RMSE), the mean absolute error (MAE), the bias (BIAS), and the maximum prediction error (MPE). To be precise, let $i_{(n)k} \leq \ldots \leq i_{(1)k}$ be the sorted annual maximum intensities for a given duration d_k. The empirical exceedance probability $p_j = P\{i > i_{(j)k}\}$, associated to the jth value $i_{(j)k}$, is usually called a plotting position and can be written as $p_j = (j-a)/(n+1-2a)$ for some value of a in the range from 0 to 0.5. As concluded in Guo (1990), Cunanne's plotting position (a=0.4) is reasonable for the GEV distribution. Accordingly, the empirical return period of $i_{(j)k}$ is $T_j = 1/p_j$. Then $i_{(j)k}$ can therefore be compared with the posterior mean of the T_j-year return level, here denoted by $\bar{i}_{T_j,k} =: \bar{i}_{jk}$. For each duration d_k, the scores take the form

$$\begin{aligned} \mathrm{RMSE}_k &= \left[\frac{1}{n}\sum_{j=1}^{n}\left(i_{(j)k}-\bar{i}_{jk}\right)^2\right]^{1/2}, \quad \mathrm{MAE}_k = \frac{1}{n}\sum_{j=1}^{n}\left|i_{(j)k}-\bar{i}_{jk}\right|, \\ \mathrm{BIAS}_k &= \frac{1}{n}\sum_{j=1}^{n}\left(i_{(j)k}-\bar{i}_{jk}\right), \qquad \mathrm{MPE}_k = \max_{j\in\{1,\cdots,n\}}\left|i_{(j)k}-\bar{i}_{jk}\right|. \end{aligned} \tag{49}$$

Because the magnitude of the intensities can be very different for different durations, a meaningful comparison of the model performance among the considered durations can be made by normalizing the scores with the mean of the observations. This is the coefficient of variation (CV) of the scores:

$$\mathrm{CV}(\mathrm{RMSE}_k) = \frac{\mathrm{RMSE}_k}{\frac{1}{n}\sum_{j=1}^{n} i_{jk}}, \tag{50}$$

and so forth. Figure 8 displays the CV of the scores as a function of the rainfall duration. We applied the two GEV models (simple scaling and multiscaling-based) and the multifractal marginal and hybrid (MFM/H) method of Veneziano et al. (2007). A particular gain is achieved with the multiscaling-based model for short rainfall durations (1–3 hr) and for longer durations (≥12 hr). As we already concluded from Figure 6, both GEV models behave similarly for durations 6–12 hr. The MFM/H method is nearly unbiased, but the RMSE, MAE, and MPE are generally higher than those of the multiscaling-based model. For rainfall durations between 4 and 20 hr, the MFM/H method performs better than the simple scaling model (excluding MPE). However, a more valuable comparison by means of information criteria is not possible because they are only applicable for models using exact the same data. The GEV models use annual maxima data, whereas the MFM/H method is based on the initial or parent distribution. In addition, the MFM/H method does not include likelihood-based inference, which is necessary for the use of information criteria. Hence, a valuable comparison is difficult.

7 | CONCLUSIONS

It is found that the multiscaling hypothesis describes the IDF characteristics of Belgian rainfall. Two multiscaling-based GEV models for the annual maximum d-hourly intensity were proposed: (a) an exact multiscaling GEV model, where the parameters are expressed as a function of the multiscaling mean and variance, and (b) a simplified GEV model, which is multiscaling to an excellent extent, but not exactly. Specifically, the location and scale parameters of GEV model (b) are related through the power laws $d^{-\eta_1}$ and $d^{-\eta_2}$, respectively, with $\eta_1 \leq \eta_2$, for rainfall durations of 1 up to 72 hr. It extends the simple scaling GEV model for which $\eta_1 = \eta_2$ (Menabde et al., 1999; Nguyen et al., 1998).

The motivation to search for a simplified version (b) was that the estimation problem of the original version (a) is ill-posed. In addition, model (b) slightly better fits than model (a). This might encourage further research on non-multifractal modelling alternatives.

As well known, the simple scaling GEV model leads to a specific IDF relationship of the form, Equation 1, compare Koutsoyiannis et al. (1998), which satisfies the separability condition. In contrast, the multiscaling-based IDF relationship is not a separable function of d and T. Because the new IDF relationship contains only five parameters, it should prove quite useful to people who need to model extreme intensities in a parsimonious manner.

The Bayesian scheme looks rather complicated. If only one single value of the IDF parameters is required (without confidence/credible intervals), one can use a simple point estimator such as the typical procedure, or the one-step least square method of Koutsoyiannis et al. (1998). For the general IDF relationship, it was concluded in Van de Vyver (2015a) that these point estimators agree very well with the posterior means. An extension to the multiscaling-based GEV model is straightforward.

The multiscaling-based GEV model and the Bayesian estimation method are clarified with an application by using 10-min rainfall data. An analysis of a 110-year time series at Uccle (Belgium) is carried out to clearly illustrate the theory. Additional records of maximum intensities in Belgium, with a more realistic amount of data (31–38 years), were also analysed to support the application of the multiscaling-based GEV model. Overall, model comparison with information criteria confirms that the multiscaling-based GEV model should be preferred over the simple scaling version.

Presently, we have no clue in which climatic regions the new model is applicable and in which region the simple scaling model should be considered. More analysis and more data are needed to identify the IDF characteristics worldwide. However, short-duration rainfall series (e.g., 5 and 10 min) are difficult to obtain.

An important extension would be to employ the peaks-over-threshold method in the IDF analysis, which includes more data than the GEV methodology. As a result, smaller uncertainty into return level prediction is to be expected. To our knowledge, the only IDF relationship in existence whose specific form is explicitly derived from the peaks-over-threshold methodology is given in Willems (2000). A further investigation on the applicability of the present framework to the peaks-over-threshold method would be highly desirable.

ACKNOWLEDGMENT

URCLIM has received funding from EU's H2020 Research and Innovation Program under Grant Agreement 690462.

ORCID

Hans Van de Vyver http://orcid.org/0000-0001-7142-4693

REFERENCES

Bernardo, J. M., & Smith, A. F. M. (1994). *Bayesian theory*. Chichester: Wiley.

Bougadis, J., & Adamowski, K. (2006). Scaling model of a rainfall intensity–duration–frequency relationship. *Hydrological Processes*, *20*, 3747–3757.

Burlando, P., & Rosso, R. (1996). Scaling and multiscaling models of depth–duration–frequency curves for storm precipitation. *Journal of Hydrology*, *187*, 45–64.

Chandler, R. E., & Bate, S. (2007). Inference for clustered data using the independence loglikelihood. *Biometrika*, *94*, 167–183.

Coles, S. (2001). *An introduction to statistical modeling of extreme values*. Heidelberg: Springer-Verlag.

Davison, A. C. (2003). *Statistical models*. Cambridge: Cambridge University Press.

Demarée, G. R. (2003). Le pluviographe centenaire du plateau d'Uccle: son histoire, ses données et ses applications. *La Houille Blanche*, *4*, 1–8.

Durrans, S. R. (2010). Intensity–duration–frequency curves. In F. Y. Testik, & M. Gebremichael (Eds.), *Rainfall: State of the Science* (pp. 159–169). Washington, DC: American Geophysical Union.

Gao, X., & Song, P. X.-K. (2010). Composite likelihood Bayesian information criteria for model selection in high dimensional data. *Journal of the American Statistical Association*, *105*, 1531–1540.

Gelman, A., Carlin, J. B., Stern, H. S., Dunson, D. B., Vehtari, A., & Rubin, D. B. (2013). *Bayesian data analysis* (third edition). Boca Raton, London, New York Washington, D.C: Chapman & Hall/CRC.

Guo, S. L. (1990). A discussion on unbiased plotting positions for the general extreme value distribution. *Journal of Hydrology*, *121*, 33–44.

Gupta, V. K., & Waymire, E. (1990). Multiscaling properties of spatial rainfall and river flow distributions. *Journal of Geophysical Research*, *95*, 1999–2009.

Kent, J. T. (1982). Robust properties of likelihood ratio test. *Biometrika*, *69*, 19–27.

Koutsoyiannis, D., Kozonis, D., & Manetas, A. (1998). A mathematical framework for studying rainfall intensity–duration–frequency relationships. *Journal of Hydrology*, *206*, 118–135.

Langousis, A., & Veneziano, D. (2007). Intensity–duration–frequency curves from scaling representations of rainfall. *Water Resources Research*, *43*, W02422.

Leadbetter, M. R., Lindgren, G., & Rootzén, H. (1983). *Extremes and related properties of random sequences and processes*. New York: Springer.

Menabde, M., Seed, A., & Pegram, G. (1999). A simple scaling model for extreme rainfall. *Water Resources Research*, *35*, 335–339.

Nguyen, V. T. V., Nguyen, T. D., & Wang, H. (1998). Regional estimation of short duration rainfall extremes. *Water Science and Technology*, *37*, 15–19.

Papalexiou, S. M., & Koutsoyiannis, D. (2013). Battle of extreme value distributions: A global survey on extreme daily rainfall. *Water Resources Research*, *49*, 187–201.

Pauli, F., Racugno, W., & Ventura, L. (2011). Bayesian composite marginal likelihoods. *Statistica Sinica*, *21*, 149–164.

Ribatet, M., Cooley, D., & Davison, A. C. (2012). Bayesian inference from composite likelihoods, with an application to spatial extremes. *Statistica Sinica*, *22*, 813–845.

Spiegelhalter, D. J., Best, N. G., Carlin, B. P., & van der Linde, A. (2002). Bayesian measures of model complexity and fit. *Journal of the Royal Statistical Society. Series B*, *64*, 583–639.

Van de Vyver, H. (2015a). Bayesian estimation of rainfall intensity–duration–frequency relationships. *Journal of Hydrology*, *529*, 1451–1463.

Van de Vyver, H. (2015b). On the estimation of continuous 24-h precipitation maxima. *Stochastic Environmental Research and Risk Assessment*, *29*, 653–663.

Varin, C., & Vidoni, P. (2005). A note on composite likelihood inference and model selection. *Biometrika*, *92*, 519–528.

Varin, C., Reid, N., & Firth, D. (2011). An overview of composite likelihoods. *Statistica Sinica*, *21*, 5–42.

Veneziano, D., & Furcolo, P. (2002). Multifractality of rainfall and scaling of intensity–duration–frequency curves. *Water Resources Research*, *38*, 1306.

Veneziano, D., Lepore, C., Langousis, A., & Furcolo, P. (2007). Marginal methods of intensity–duration–frequency estimation in scaling and nonscaling rainfall. *Water Resources Research*, *43*, W10418.

Veneziano, D., & Yoon, S. (2013). Rainfall extremes, excesses, and intensity–duration–frequency curves: A unified asymptotic framework and new nonasymptotic results based on multifractal measures. *Water Resources Research*, *49*, 4320–4334.

Willems, P. (2000). Compound intensity/duration/frequency-relationships of extreme precipitation for two seasons and two storm types. *Journal of Hydrology*, *233*, 189–205.

Yu, P.-S., Yang, T.-C., & Lin, C.-S. (2004). Regional rainfall intensity formulas based on scaling property of rainfall. *Journal of Hydrology*, *295*, 108–123.

How to cite this article: Van de Vyver H. A multiscaling-based intensity–duration–frequency model for extreme precipitation. *Hydrological Processes*. 2018;32:1635–1647. https://doi.org/10.1002/hyp.11516